Online-Journals.org

iJOE International Journal of Online and Biomedical Engineering

iJOE | eISSN: 2626-8493 | Vol. 22 No. 11 (2026) | OPEN ACCESS

https://doi.org/10.3991/ijoe.v22i11.62219

PAPER

A BLE-Based IMU System with Three-Stage Calibration and Madgwick Sensor Fusion for Real-Time Orientation Tracking

Shujiang Zhang[1], Md. Mahmudur Rahman[1,2], Xuejin Cao[1], Kok Beng Gan[1] (✉), Kok Swee Sim[3]

[1]Universiti Kebangsaan Malaysia, Selangor, Malaysia

[2]Daffodil International University, Dhaka, Bangladesh

[3]Multimedia University, Malacca, Malaysia

kbgan@ukm.edu.my

ABSTRACT

This paper presents a prototype wireless IMU-based motion tracking system for real-time orientation estimation. Each wearable node integrates an MPU9250 IMU with a Nordic nRF52832 microcontroller, enabling concurrent multi-node communication via Bluetooth Low Energy (BLE). To improve measurement accuracy, a three-stage calibration framework consisting of accelerometer and gyroscope zero-offset calibration and magnetometer ellipsoid fitting is applied to compensate for sensor bias, drift, and magnetic interference. The Madgwick algorithm estimates yaw, pitch, and roll from the calibrated data, which are transmitted via the Nordic UART Service (NUS) and visualized in real time using a Python application based on Bleak and OpenGL. Experimental validation with 30 healthy volunteers demonstrated reliable multi-node communication with an end-to-end latency below 50 ms and accurate orientation measurement. Comparison with a clinical goniometer yielded a Pearson correlation coefficient of $r = 0.9999$ ($p < 0.001$) and Bland–Altman 95% limits of agreement (LoA) of ±3.99°. Although evaluated only under static uniaxial conditions in healthy participants, the proposed system demonstrated strong agreement with the reference measurements, highlighting its potential as a wearable, low-cost solution for rehabilitation angle monitoring.

KEYWORDS

Bluetooth Low Energy (BLE), Inertial Measurement Unit (IMU), Madgwick filter, ellipsoid fitting, sensor fusion, orientation, rehabilitation

1 INTRODUCTION

Inertial Measurement Units (IMUs) play a crucial role in motion capture and sensor fusion, significantly enhancing the accuracy and reliability of motion tracking systems across diverse applications, including virtual reality and biomechanics. IMUs integrate accelerometers, gyroscopes, and magnetometers to provide real-time

Zhang, S., Rahman, M. M., Cao, X., Gan, K. B., Sim, K. S. (2026). A BLE-Based IMU System with Three-Stage Calibration and Madgwick Sensor Fusion for Real-Time Orientation Tracking. *International Journal of Online and Biomedical Engineering (iJOE)*, 22(11), pp. 157–171. https://doi.org/10.3991/ijoe.v22i11.62219

Article submitted 2026-05-04. Revision uploaded 2026-07-20. Final acceptance 2026-07-21.

© 2026 by the authors of this article. Published under CC-BY.

data on linear and angular motion, enabling precise tracking of body movements for applications in rehabilitation and sports science [1–3]. Unlike traditional optical motion capture systems, which are restricted to controlled environments, IMUs offer the flexibility to operate in diverse settings, including home-based rehabilitation and outdoor sports [1, 4, 5]. This adaptability is particularly advantageous in scenarios with limited visibility, such as indoor spaces or adverse weather conditions [4, 6].

Studies have demonstrated that IMUs can achieve accuracy comparable to optical systems. A previous validation study established the Valor IMU system as a reliable alternative to optical motion capture, reporting mean absolute differences in joint angles between 1.81° and 17.46° [1]. Similarly, the Perception Neuron system achieved a root mean square error (RMSE) of less than 4° for joint angles, validating its suitability for dynamic movement tracking [7]. IMU sensor drift can introduce cumulative errors in position and orientation estimates, a problem that becomes particularly pronounced during rapid movements or under dynamic conditions [8]. While calibration routines are essential for minimizing these errors, they are often complex and time-consuming [9–10]. To overcome these challenges, advanced sensor fusion techniques such as Kalman and complementary filters are employed. By integrating measurements from multiple sensors, these algorithms mitigate drift, enhance data reliability, and improve overall motion tracking performance [11–12].

IMUs are also susceptible to external factors such as magnetic interference, which can distort measurements. Therefore, proper calibration and controlled environmental conditions are essential for ensuring reliable performance [10, 13]. From a practical standpoint, IMUs are generally more cost-effective than optical systems, making them accessible for a broader range of applications, including consumer-level products [4, 7]. Their compact size and wireless capabilities facilitate streamlined set-up and deployment across various environments, in contrast to bulky optical systems that require extensive calibration and infrastructure [4, 6]. Concurrently, improved calibration techniques are being developed to further enhance measurement accuracy and reliability [14–16]. The future of IMUs in motion capture is promising, with potential integration into smart devices, drones, and robotics, which could enable more sophisticated applications in fields such as autonomous navigation and human–robot interaction [12, 15].

Inertial Measurement Units and Bluetooth Low Energy (BLE) technology are increasingly being integrated into rehabilitation practices, enhancing patient outcomes, facilitating remote monitoring, and creating personalized rehabilitation programs. By continuously monitoring patient movements and providing real-time feedback, clinicians can adjust therapy based on individual progress and needs [17–18]. Personalized approaches supported by IMU and BLE data have been shown to improve patient outcomes, such as mobility and functional independence. For instance, a system that estimates spinal angles during rehabilitation exercises demonstrated high accuracy and could be implemented for home-based therapy, increasing accessibility [19–22]. The integration of IMUs and BLE technology in rehabilitation offers promising applications for enhancing patient outcomes through detailed movement analysis, remote monitoring, and personalized interventions [23–25]. Recent systems leverage multi-sensor fusion and mobile interaction to provide patients with real-time feedback during exercises [26]. However, addressing the technical and usability challenges is crucial for maximizing the efficacy of these technologies in clinical practice.

This study aims to develop and validate a real-time sensor fusion framework that minimizes cumulative drift in wireless IMU systems during rehabilitation exercises while maintaining a calibration process sufficiently lightweight for non-expert users in both clinical and home-based settings.

2 METHODOLOGY

2.1 System architecture

The developed wireless motion sensing system consists of multiple wearable IMU nodes and a centralized host unit for real-time processing and visualization (see Figure 1). Each IMU node integrates an InvenSense MPU-9250 sensor with a Nordic nRF52832 microcontroller on a custom-designed compact PCB, incorporating MX25R80 flash memory and a rechargeable battery for portable operation. The MPU-9250 provides 9-axis motion sensing through a tri-axial accelerometer, gyroscope, and magnetometer. The nRF52832, featuring an ARM Cortex-M4F processor, 512 kB Flash memory, and 64 kB RAM, provides sufficient computational capability and energy efficiency for wearable data processing and BLE communication [27]. Firmware development was performed using Keil µVision 5, with debugging supported by a SEGGER J-Link interface.

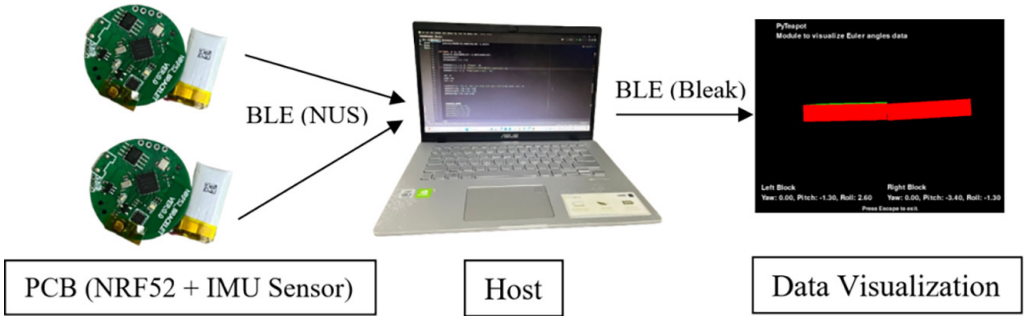


Fig. 1. Wireless motion sensing system design

Each node transmits sensor data wirelessly via BLE using the Nordic UART Service (NUS), which provides serial-like communication through custom 128-bit UUID characteristics. An nRF52840 USB dongle functions as the BLE central device and interfaces with the host computer. A Python-based application developed in the PyCharm environment utilizes the Bleak library for BLE communication and OpenGL/Pygame for real-time visualization. The PyTeapot module renders the estimated orientation as a 3D cube representation. Each data packet contains a timestamp to ensure temporal synchronization among multiple IMU nodes. The host application performs stream synchronization through timestamp-based interpolation, enabling coherent multi-sensor analysis. The system operates at a sampling rate of 50–100 Hz with an end-to-end latency below 50 ms.

2.2 Wireless communication protocol

Wireless communication between the IMU nodes and the host device was implemented using the NUS, a BLE GATT-based service that emulates serial communication over a wireless link. NUS was selected due to its simplicity, reliability, and compatibility with Nordic Semiconductor platforms, enabling efficient bidirectional data exchange without requiring a custom communication protocol. The service consists of two GATT characteristics: the TX characteristic (UUID: 6E400003-B5A3-F393-E0A9-E50E24DCCA9E), which enables IMU nodes to transmit sensor data to the central host device, and the RX characteristic (UUID: 6E400002-B5A3-F393-E0A9-E50E24DCCA9E),

which allows the host to send commands or configuration parameters to the nodes. The TX characteristic utilizes the notification property, while the RX characteristic employs the write property, enabling asynchronous event-driven communication with reduced polling overhead.

Each orientation update transmitted by the IMU node is encapsulated in a 12-byte payload consisting of three 32-bit IEEE 754 single-precision floating-point values representing roll, pitch, and yaw angles in radians. The data are encoded using little-endian byte ordering, consistent with the ARM Cortex-M4F architecture. Table I presents the packet structure of the developed wireless IMU-based motion tracking system.

Table 1. Packet structure of the IMU sensor

Byte Offset	Field	Size (bytes)	Data Type	Description
0–3	Roll	4	float32	Rotation around the x-axis (rad)
4–7	Pitch	4	float32	Rotation around the y-axis (rad)
8–11	Yaw	4	float32	Rotation around the z-axis (rad)

Figure 2 illustrates the end-to-end timing sequence for a single 12-byte orientation data transmission. The IMU firmware samples the MPU9250 at 100 Hz and performs calibration and Madgwick sensor fusion within the 10 ms sampling period. The estimated roll, pitch, and yaw values are then encoded into the payload and transmitted through the NUS TX characteristic. Following the BLE connection interval of 7.5 ms, the notification is delivered over the wireless link with an approximate propagation delay of 2.5 ms. Upon reception, the host decodes the three float32 values and forwards the orientation data to the OpenGL renderer. The overall latency from sensor acquisition to visualization is approximately 20 ms, demonstrating the suitability of the system for real-time rehabilitation monitoring.

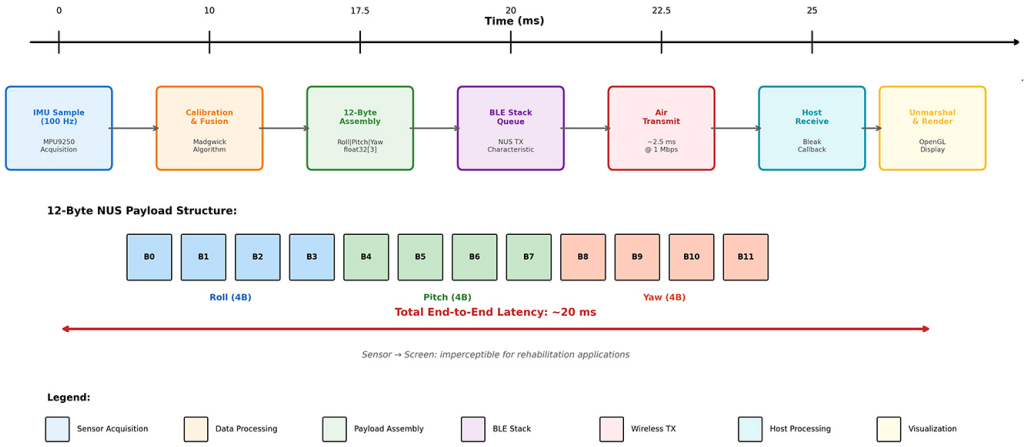


Fig. 2. NUS end-to-end timing diagram for 12-byte orientation data transmission

On the host device, the Python application utilizes the Bleak library to discover advertising IMU peripherals, establish BLE connections, and enable notifications on the NUS TX characteristic. Upon receiving each 12-byte notification, an asynchronous callback function decodes the little-endian float32 values, converts the orientation data from radians to degrees, and forwards the results to the PyTeapot OpenGL renderer for real-time 3D visualization.

For upper-limb rehabilitation applications requiring simultaneous tracking of the forearm and upper arm, the host application maintains two independent BLE connections with separate IMU nodes. Each connection is managed through an independent asynchronous task within the Python asyncio framework, enabling non-blocking data acquisition from both sensors. The MAC addresses of the IMU nodes are pre-configured to support automatic reconnection without manual pairing. Received orientation streams are timestamped using the host system clock with millisecond resolution, enabling synchronization analysis and elbow joint angle estimation through differential pitch calculation.

2.3 Sensor calibration

During static accelerometer calibration, the sensor was placed in a known orientation with the z-axis aligned with gravity. The expected acceleration vector, estimated offset, and the calibrated accelerometer measurement were then calculated using Eq. (1), Eq. (2), and Eq. (3), respectively.

$$\boldsymbol{a}_{ref} = [\mathbf{0},\mathbf{0},\mathbf{1}\boldsymbol{g}]^T \tag{1}$$

$$\boldsymbol{b}_a = \frac{\mathbf{1}}{\boldsymbol{N}} \sum_{\boldsymbol{i}=\mathbf{1}}^{\boldsymbol{N}} \boldsymbol{a}_i - \boldsymbol{a}_{ref} \tag{2}$$

$$\boldsymbol{a}_{c,i} = \boldsymbol{a}_i - \boldsymbol{b}_a \tag{3}$$

where $\boldsymbol{a}_i$ is the raw accelerometer vector at sample $\boldsymbol{i}$, $\boldsymbol{N}$ is the number of static samples, and $\boldsymbol{b}_a$ is the estimated accelerometer bias.

For gyroscope calibration, the sensor was kept stationary, and the expected angular velocity was zero. The gyroscope bias and calibrated gyroscope signal were calculated using Eq. (4) and Eq. (5), respectively.

$$\boldsymbol{b}_g = \frac{\mathbf{1}}{\boldsymbol{N}} \sum_{\boldsymbol{i}=\mathbf{1}}^{\boldsymbol{N}} \boldsymbol{\omega}_i \tag{4}$$

$$\boldsymbol{\omega}_{c,i} = \boldsymbol{\omega}_i - \boldsymbol{b}_g \tag{5}$$

where $\boldsymbol{\omega}_i$ is the raw gyroscope measurement.

For magnetometer calibration, ellipsoid fitting was used to compensate for hard-iron and soft-iron distortions as in Eq. (6).

$$\boldsymbol{m}_{c,i} = \boldsymbol{S}(\boldsymbol{m}_{r,i} - \boldsymbol{b}_m) \tag{6}$$

where $\boldsymbol{m}_{r,i}$ is the raw magnetometer vector, $\boldsymbol{b}_m$ is the hard-iron bias vector, and $\boldsymbol{S}$ is the soft-iron compensation matrix estimated from ellipsoid fitting.

2.4 Sensor fusion and orientation estimation

The Madgwick filter fuses accelerometer, gyroscope, and magnetometer data for stable orientation estimation. It reduces gyroscope integration drift using gradient-descent corrections that minimize errors between measured and estimated

gravity and magnetic field vectors, thereby updating the quaternion continuously, as shown in Eq. (7).

$$\boldsymbol{q} = \frac{1}{2}\boldsymbol{q} \otimes \boldsymbol{\omega} - \beta \nabla \boldsymbol{f}(\boldsymbol{q}, \boldsymbol{a}, \boldsymbol{m}) \tag{7}$$

where $\boldsymbol{q}$ is the orientation quaternion, $\boldsymbol{\omega}$ is the angular velocity from the gyroscope, $\boldsymbol{\beta}$ is the filter gain controlling drift correction strength, and $\nabla \boldsymbol{f}(\boldsymbol{q},\boldsymbol{a},\boldsymbol{m})$ is the gradient of the objective function based on accelerometer (a) and magnetometer (m) measurements.

The Madgwick filter mitigates gyroscope integration drift by incorporating accelerometer measurements as a gravity reference and magnetometer data as a heading reference, thereby stabilizing the orientation estimate. The resulting orientation is represented in quaternion form and subsequently converted into Euler angles for interpretation as shown in Eq. (8–10). Specifically, roll (φ), pitch (θ), and yaw (ψ) correspond to rotations about the x-, y-, and z-axes, respectively, and are computed from the quaternion components using (7).

$$\varphi = atan2(2q_3q_4 - 2q_1q_2, 2q_1^2 - 1 + 2q_4^2) \tag{8}$$

$$\theta = -asin(2q_2q_4 + 2q_1q_3) \tag{9}$$

$$\psi = atan2(2q_2q_3 - 2q_1q_4, 2q_1^2 - 1 + 2q_2^2) \tag{10}$$

2.5 Experimental protocol

Thirty healthy adult volunteers were recruited through simple random sampling from the staff and student population of Universiti Kebangsaan Malaysia (UKM). Participants were included if they had no known neuromuscular, musculoskeletal, or joint-related disorders affecting upper-limb movement. The study protocol was approved by the UKM Research Ethics Committee (JEP-2025-170).

Elbow joint kinematics were simultaneously measured using the proposed IMU system and a clinical analog goniometer as the reference standard. The IMU node was securely attached to the target limb segment and aligned with the anatomical axis of rotation. Before each trial, the sensor was initialized in a static posture to minimize orientation offset and drift. Each participant performed three repeated flexion and extension trials under supervision, during which IMU angular data were continuously recorded while the corresponding end-range joint angles were measured using a goniometer by a trained operator. Rest intervals were provided between trials to reduce fatigue-related variability.

The agreement, accuracy, and reliability between the IMU and goniometer measurements were evaluated using RMSE, Pearson correlation coefficient (R), and Bland–Altman analysis. RMSE was used to quantify measurement deviation, while Pearson correlation assessed the linear relationship between the two systems. Bland–Altman analysis was performed to determine measurement bias and the 95% limits of agreement (LoA), providing an assessment of systematic differences and agreement between methods. Correlation and Bland–Altman plots were generated to support statistical interpretation.

3 RESULTS AND DISCUSSION

3.1 Real-time visualization

The Python-based application was designed to support real-time data visualization from multiple concurrent data sources. It leverages the Bleak library to scan for and identify multiple BLE devices via their unique MAC addresses, establishing simultaneous connections to several wireless IMU sensors. Once connected, the system continuously collects orientation data, including yaw, pitch, and roll angles, from each sensor in parallel. Each sensor's orientation is rendered as an individual, interactive three-dimensional model on the display, with the real-time rotational movements of the physical sensors accurately mirrored in their corresponding digital representations as shown in Figure 3. This multi-view visualization framework provides clinicians and researchers with a dynamic, intuitive interface for monitoring and comparing sensor orientations across multiple body segments during rehabilitation exercises.

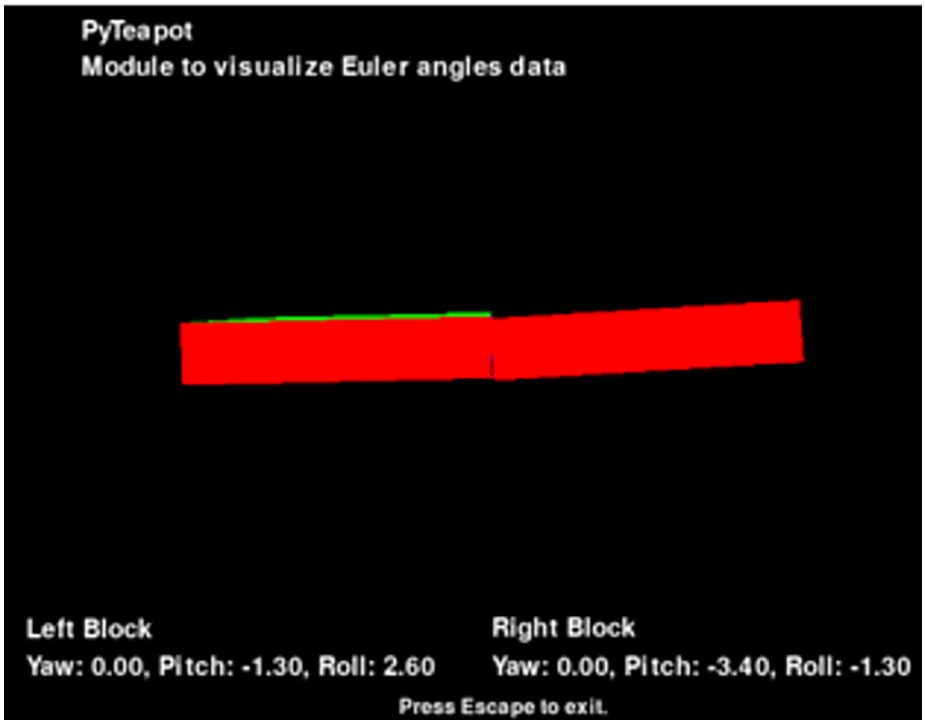


Fig. 3. Data visualization in Python

3.2 Calibration performance

To calibrate the accelerometer data, the three-axis IMU sensor was placed in a static condition and horizontally on a flat surface. In the raw data, the X-axis shows a slight positive offset near zero, the Y-axis exhibits a more noticeable offset of approximately 0.08 g, and the Z-axis reads around 1.0 g with visible high-frequency noise superimposed on the signal. These offsets in the X and Y axes represent static bias errors that deviate from the expected zero-g reading when the sensor

is horizontal, while the Z-axis correctly measures the gravitational acceleration but suffers from measurement noise. After applying calibration, the compensated data shows significant improvement: both the X and Y axes are now accurately centered at zero, eliminating the bias errors, and the Z-axis maintains its 1.0 g magnitude with notably reduced noise levels, shown in Figure 4a and 4b. This calibration effectively removes the systematic offsets and suppresses random fluctuations, resulting in cleaner signals that are essential for reliable motion tracking in rehabilitation applications where precise acceleration measurements directly impact the accuracy of joint angle estimation and movement analysis.

To do the gyroscope calibration, the three-axis IMU sensor was kept in a stationary condition. In the raw data, all three axes exhibit significant bias offsets and high-amplitude noise: the X-axis centers around approximately 1.2–1.3 units, the Y-axis hovers near 0.1–0.2 units, and the Z-axis reads around 0.6–0.7 units, with all axes showing fluctuations spanning roughly ±0.5 units. Since the sensor is stationary, the ideal gyroscope reading should be zero across all axes, as no rotational motion is occurring; however, the raw data clearly deviates from this expected behavior due to inherent sensor biases and noise. After applying calibration, the compensated data demonstrates substantial improvement: all three axes are now centered much closer to zero, with most values falling within the ±0.2 range, and the large static offsets previously observed in the X and Z axes are effectively eliminated, which is shown in Figure 4c and 4d. The calibration process successfully removes the systematic bias errors and reduces the overall noise amplitude, though some residual high-frequency fluctuations remain visible. This bias correction is critical for rehabilitation applications, where even small gyroscope errors can accumulate over time during orientation estimation, leading to significant drift in computed joint angles and compromising the accuracy of movement analysis.

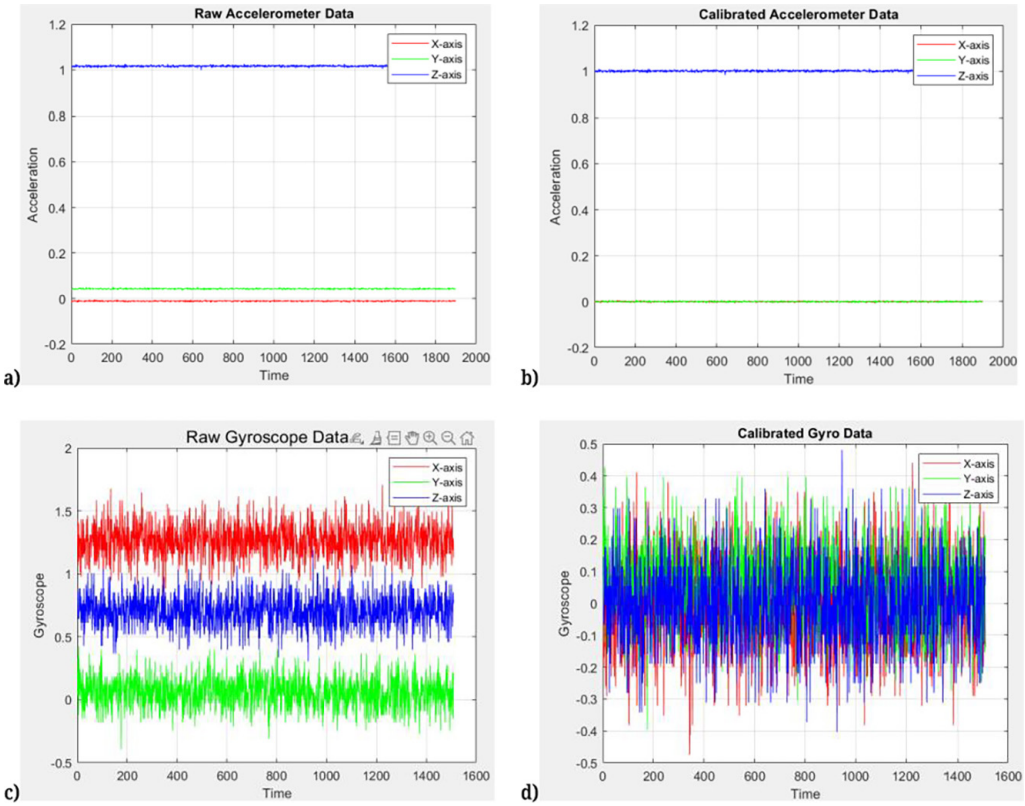


Fig. 4. Raw and calibrated accelerometer and gyroscope data

Figure 5 presents a comparison between raw and calibrated magnetometer data in a 3D scatter plot format, illustrating the critical process of magnetometer calibration for accurate magnetic field sensing. In panel (a), the raw magnetometer data appears as an ellipsoid that is both offset from the origin and scaled differently along each axis, indicating the presence of hard-iron offsets (shifting the center away from zero), soft-iron distortions (stretching the sphere into an ellipsoid), and scale factor errors (different sensitivities along the X, Y, and Z axes). Panel (b) shows the result after applying calibration parameters, where the data has been successfully transformed into a unit sphere centered at the origin, demonstrating that the hard-iron biases have been removed, the ellipsoid has been corrected to a sphere, and the scale has been normalized. This calibration is essential in IMU applications because uncorrected magnetometer errors would introduce significant heading inaccuracies when fusing magnetometer data with accelerometer and gyroscope measurements for orientation estimation.

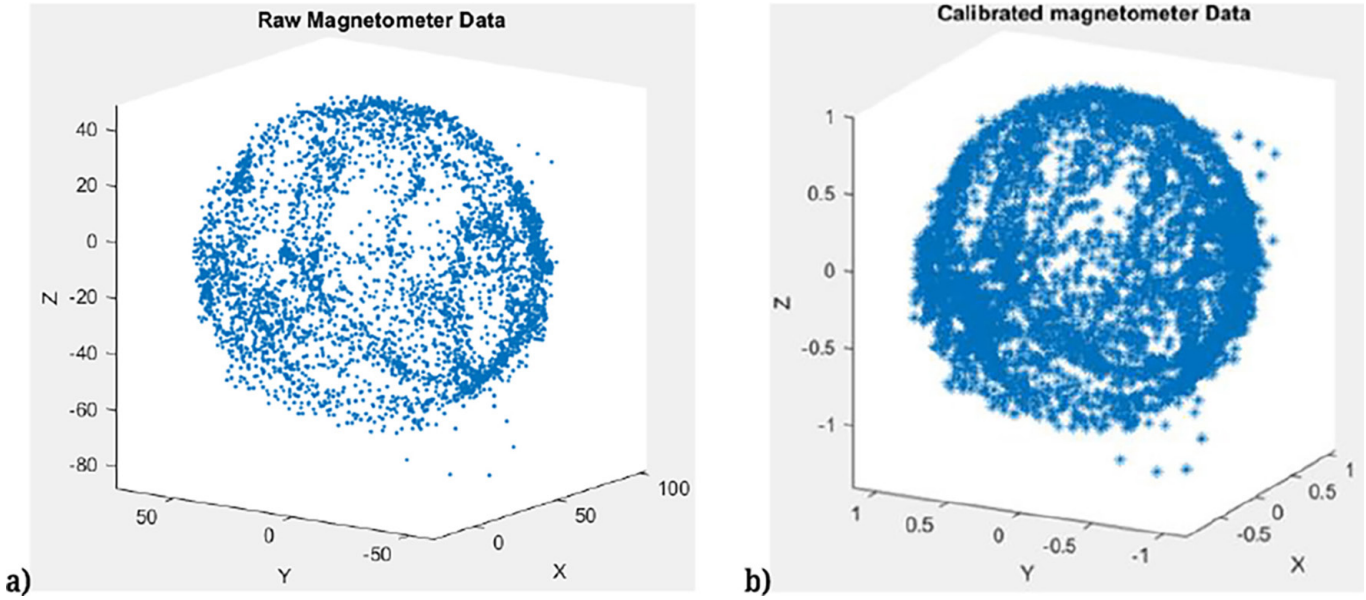


Fig. 5. Raw and calibrated magnetometer data

3.3 Statistical data analysis

This study compares IMU sensor measurements and goniometer measurements for two types of joint movement: extension and flexion. For extension, the IMU records an average of about 177°, whereas the goniometer shows a slightly lower average of 175.6°, indicating that the IMU tends to slightly overestimate extension angles. For flexion, the IMU measures around 31.9°, while the goniometer records 33.8°, showing that the IMU slightly underestimates flexion angles. Figure 6 presents the (Mean ± SD) comparison between IMU vs Goniometer. On the x-axis, the two conditions are shown, while the y-axis represents the angle in degrees, ranging from 0 to 200°. The error bars on each bar are small, suggesting consistent measurements across trials. Overall, the graph highlights that IMU readings are closely aligned with goniometer values, with minimal error in extension and modest underestimation in flexion.

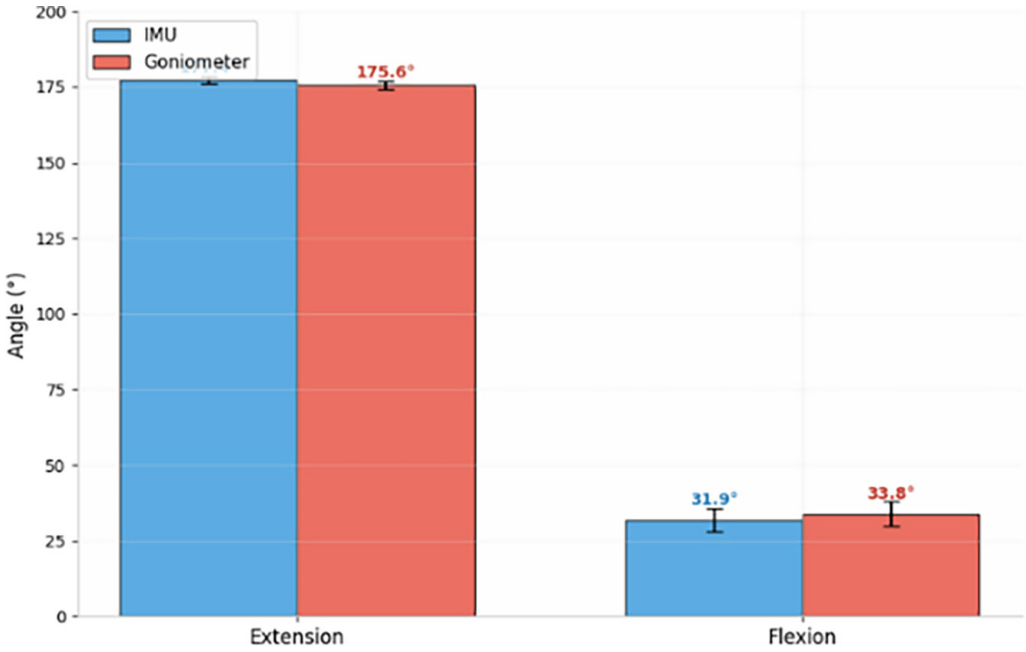


Fig. 6. Mean ± SD comparison between IMU vs. Goniometer

The IMU measurements showed a very strong relationship and close agreement with the goniometer measurements for both extension and flexion movements. The correlation analysis indicated that the IMU closely followed the goniometer values, with only a slight systematic bias. As shown in Figure 7a, the regression equation was ($y = 1.026x - 2.730$), with ($r = 0.9999$), ($p < 0.001$), and ($R^2 = 0.9999$). The x-axis represents goniometer readings, and the y-axis represents IMU readings, both in degrees, while blue and red circles indicate extension and flexion data, respectively. The dashed black line represents perfect agreement, and the solid green line shows the actual regression relationship.

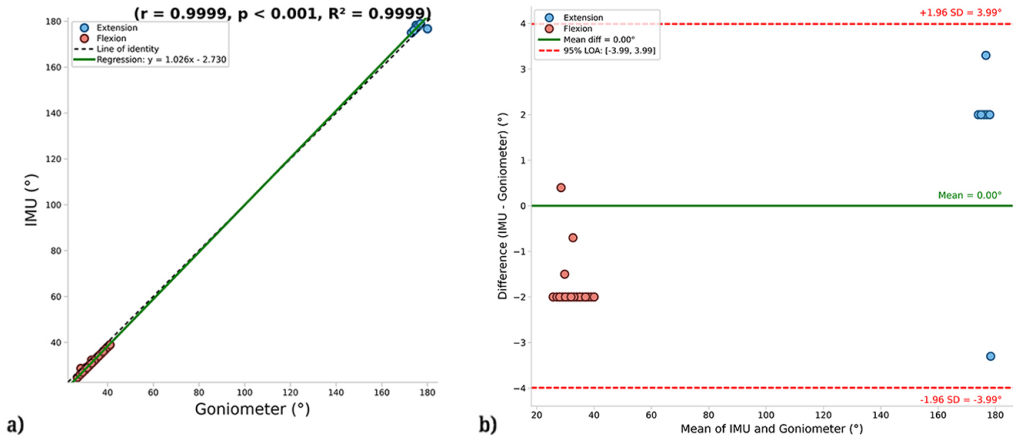


Fig. 7. Correlation test between IMU vs. Goniometer

The agreement analysis also showed minimal differences between the two measurement methods. The mean difference was approximately 0°, indicating essentially no overall systematic bias, while the 95% LoA ranged from –3.99° to +3.99°. As illustrated in Figure 7b, the x-axis represents the mean of the IMU and

goniometer measurements, and the y-axis represents their difference. Blue and red points correspond to extension and flexion movements, respectively, while the solid green line indicates the mean difference and the dashed red lines show the LoA. Nearly all data points fell within this narrow range, confirming that the IMU provides accurate, reliable, and consistent joint-angle measurements and can serve as a valid alternative to the goniometer.

Intra-trial consistency of extension and flexion angle measurements was evaluated across 30 volunteers. Extension measurements showed excellent repeatability, with the three trials clustering closely around the IMU average within an approximate range of 170°–184°. In contrast, flexion measurements, ranging from approximately 20° to 45°, generally followed the IMU average but showed greater dispersion and trial-to-trial variability. These observations agree with the coefficient of variation results, with extension demonstrating higher intra-trial reliability (CV ≈ 0.59%) than flexion (CV ≈ 3.50%). As illustrated in Figure 8, the IMU showed strong measurement stability for extension, while flexion measurements remained acceptable but exhibited comparatively greater variability across repeated trials.

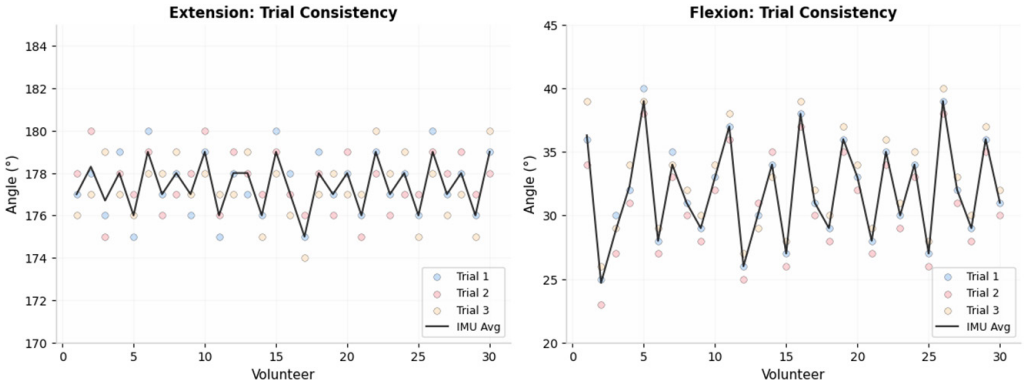


Fig. 8. Intra-trial consistency across volunteers

4 CONCLUSION

This paper presented a portable wireless motion sensor system for real-time orientation tracking in rehabilitation applications. The system integrates an MPU9250 IMU with an nRF52832 microcontroller, enabling BLE-based wireless transmission and real-time 3D visualization through a Python-based host application. A three-stage calibration framework, comprising accelerometer and gyroscope zero-offset calibration and magnetometer ellipsoid fitting, was implemented to compensate for sensor bias, drift, and magnetic interference. The Madgwick sensor fusion algorithm was employed to generate stable yaw, pitch, and roll estimates from calibrated sensor data.

Experimental validation involving 30 healthy volunteers demonstrated effective bias compensation and reliable multi-node data transmission with low latency. Comparison with a clinical goniometer yielded a Pearson correlation coefficient of $r = 0.9999$ ($p < 0.001$, $R^2 = 0.9999$), with Bland–Altman analysis showing a mean difference near 0° and 95% LoA of ±3.99°. Extension measurements exhibited excellent repeatability (CV ≈ 0.59%), while flexion showed higher variability (CV ≈ 3.50%).

The study was limited by the healthy-only cohort and evaluation under static uniaxial sagittal-plane movements. Factors including soft-tissue artifacts, sensor

misalignment, magnetic disturbances, and goniometric reference variability may contribute to measurement bias. In addition, maintaining stable multi-node BLE communication under interference and variable sampling conditions remains challenging. Future work will focus on improving synchronization and communication robustness, quantifying packet loss and sampling jitter, and validating the system in dynamic clinical rehabilitation scenarios using advanced motion capture references. Overall, the proposed BLE-based IMU system demonstrates high accuracy and reliability, supporting its potential as a portable, low-cost alternative for rehabilitation joint angle monitoring.

5 ACKNOWLEDGMENT

This work was supported by UKM under Research University Grant DIP-2024-030 and by the Ministry of Higher Education Malaysia through the Fundamental Research Grant Scheme under Grant FRGS/1/2024/TK07/UKM/02/14.

6 ETHICS STATEMENT

This study was approved by the UKM research ethics secretariat (Approval No. JEP-2025-170) and conducted in accordance with the Declaration of Helsinki. All participants provided written informed consent.

7 COMPETING INTERESTS

The authors declare no conflicts of interest.

8 DATA AVAILABILITY

The data are available from the corresponding author upon reasonable request.

9 DECLARATION OF GENERATIVE AI AND AI-ASSISTED TECHNOLOGIES IN THE WRITING PROCESS

During the preparation of this work, the authors used Kimi K2.6 instant and ChatGPT for language editing and manuscript formatting suggestions/grammatical refinement/reference style verification. After using this tool, the authors reviewed and edited the content as needed and took full responsibility for the content of the publication.

10 REFERENCES

[1] J. Smith, D. Parikh, V. Tate, S. F. Siddicky, and H.-Y. Hsiao, "Validity of valor inertial measurement unit for upper and lower extremity joint angles," *Sensors (Basel)*, vol. 24, no. 17, Art. no. 5833, 2024. https://doi.org/10.3390/s24175833

[2] J. Lourenço, L. Martins, R. Almeida, C. Quaresma, and P. Vieira, "Low cost inertial measurement unit for motion capture in biomedical applications," in *IFIP Advances in Information and Communication Technology*, Cham: Springer International Publishing, 2016, pp. 151–158. https://doi.org/10.1007/978-3-319-31165-4_16

[3] C. Gu, W. Lin, X. He, L. Zhang, and M. Zhang, "IMU-based motion capture system for rehabilitation applications: A systematic review," *Biomimetic Intelligence and Robotics*, vol. 3, no. 2, Art. no. 100097, 2023. https://doi.org/10.1016/j.birob.2023.100097

[4] M. H. Ramlee, G. K. Beng, N. Bajuri, and M. R. Abdul Kadir, "Finite element analysis of the wrist in stroke patients: The effects of hand grip," *Med. Biol. Eng. Comput.*, vol. 56, no. 7, pp. 1161–1171, 2018. https://doi.org/10.1007/s11517-017-1762-3

[5] J. Kim, L. Xie, and S. Cho, "Comparison of 3D ankle kinematics between minimal inertial measurement units configuration and optical motion capture system under diverse walking conditions," *Sci. Rep.*, vol. 16, no. 1, Art. no. 8307, 2026. https://doi.org/10.1038/s41598-026-39161-8

[6] R. Gunawan, R. Nugraha, Kusmadi, and Sukadwilinda, "Vehicle path tracking using inertial measurement unit (IMU) sensors," in *2024 18th International Conference on Telecommunication Systems, Services, and Applications (TSSA)*, 2024, pp. 1–5. https://doi.org/10.1109/TSSA63730.2024.10863844

[7] C. Z. Y. Choo, J. Y. Chow, and J. Komar, "Validation of the perception neuron system for full-body motion capture," *PLoS ONE*, vol. 17, no. 1, Art. no. e0262730, 2022. https://doi.org/10.1371/journal.pone.0262730

[8] J. Lingenberg, L. Schneider, and M. Schmidt, "Accuracy of the playermaker 2.0 IMU in tracking running distance at varying speeds in elite youth soccer," in *2025 DGON Inertial Sensors and Applications (ISA)*, 2025, pp. 1–15. https://doi.org/10.1109/ISA67150.2025.11279281

[9] J. R. A. Castillo *et al.*, "Mitigating drift in extraction of joint angle measurements from inertial measurement unit (IMU) data," in *TENCON 2024 – 2024 IEEE Region 10 Conference (TENCON)*, 2024, pp. 666–669. https://doi.org/10.1109/TENCON61640.2024.10902826

[10] M. A. Brodie, A. Walmsley, and W. Page, "The static accuracy and calibration of inertial measurement units for 3D orientation," *Comput. Methods Biomech. Biomed. Engin.*, vol. 11, no. 6, pp. 641–648, 2008. https://doi.org/10.1080/10255840802326736

[11] S. Wang and N. S. Ahmad, "A comprehensive review on sensor fusion techniques for localization of a dynamic target in GPS-denied environments," *IEEE Access*, vol. 13, pp. 2252–2285, 2025. https://doi.org/10.1109/ACCESS.2024.3519874

[12] W. Lee, P. Geneva, C. Chen, and G. Huang, "MINS: Efficient and robust multisensor-aided inertial navigation system," *J. Field Robot.*, vol. 42, no. 7, pp. 3252–3284, 2025. https://doi.org/10.1002/rob.22546

[13] I. U. Haq, F. Felicetti, D. L. Carnı', and F. Lamonaca, "Advancements in robotic positioning: A comprehensive review of measurement methods and systems," *Measur. Sens.*, vol. 45, Art. no. 102000, 2026. https://doi.org/10.1016/j.measen.2026.102000

[14] G. Chatterjee, L. Latorre, F. Mailly, P. Nouet, N. Hachelef, and C. Oudea, "Smart-MEMS based inertial measurement units: Gyro-free approach to improve the grade," *Microsyst. Technol.*, vol. 23, no. 9, pp. 3969–3978, 2017. https://doi.org/10.1007/s00542-015-2741-y

[15] M. H. Ramlee and K. B. Gan, "Function and biomechanics of upper limb in post-stroke patients-a systematic review," *J. Mech. Med. Biol.*, vol. 17, no. 6, Art. no. 1750099, 2017. https://doi.org/10.1142/S0219519417500993

[16] M. Nazarahari and H. Rouhani, "40 years of sensor fusion for orientation tracking via magnetic and inertial measurement units: Methods, lessons learned, and future challenges," *Inf. Fusion*, vol. 68, pp. 67–84, 2021. https://doi.org/10.1016/j.inffus.2020.10.018

[17] C.-L. Thouant *et al.*, "Compensation strategies in post-stroke individuals: Insights from upper body kinematics analysis based on inertial sensors," *Sensors (Basel)*, vol. 25, no. 24, Art. no. 7609, 2025. https://doi.org/10.3390/s25247609

[18] A. Shenoy *et al.*, "Evaluating the usability of inertial measurement units for measuring and monitoring activity post-stroke: A scoping review," *Sensors (Basel)*, vol. 25, no. 12, Art. no. 3694, 2025. https://doi.org/10.3390/s25123694

[19] H. Pan *et al.*, "Automated, IMU-based spine angle estimation and IMU location identification for telerehabilitation," *J. Neuroeng. Rehabil.*, vol. 21, no. 1, Art. no. 96, 2024. https://doi.org/10.1186/s12984-024-01366-1

[20] X. Y. Lim, K. B. Gan, and N. A. Abd Aziz, "Deep ConvLSTM network with dataset resampling for upper body activity recognition using minimal number of IMU sensors," *Appl. Sci. (Basel)*, vol. 11, no. 8, Art. no. 3543, 2021. https://doi.org/10.3390/app11083543

[21] M. M. Rahman, K. B. Gan, N. A. A. Aziz, A. Huong, and H. W. You, "Upper limb joint angle estimation using wearable IMUs and personalized calibration algorithm," *Mathematics*, vol. 11, no. 4, Art. no. 970, 2023. https://doi.org/10.3390/math11040970

[22] M. M. Rahman, K. B. Gan, Y. H. Woon, N. A. A. Aziz, A. Huong, and K. S. Sim, "Assessment of upper body kinematic using multiple inertial measurement units," *IEEE Sens. J.*, vol. 25, no. 6, pp. 9467–9477, 2025. https://doi.org/10.1109/JSEN.2025.3534800

[23] D. Li, K. B. Gan, and K. S. Sim, "Numerical simulation-based design of a pneumatic finger rehabilitation robot for Tele-rehabilitation," *Int. J. Online Biomed. Eng.*, vol. 22, no. 4, pp. 123–139, 2026. https://doi.org/10.3991/ijoe.v22i04.59455

[24] J.-H. Lin, "A wearable strain sensor based on 3D silicone printing with composite structure design," *Int. J. Online Biomed. Eng.*, vol. 22, no. 3, pp. 58–72, 2026. https://doi.org/10.3991/ijoe.v22i03.59657

[25] T. N. Muslim and H. A. Lafta, "Modification of an IMU based system for analyzing hand kinematics during activities of daily living," *Int. J. Online Biomed. Eng.*, vol. 19, no. 15, pp. 34–49, 2023. https://doi.org/10.3991/ijoe.v19i15.43061

[26] Y. Liu and X. Yi, "A multi-sensor fusion approach for music rhythm-based rehabilitation system with mobile interaction," *Int. J. Interact. Mob. Technol.*, vol. 20, no. 2, pp. 116–130, 2026. https://doi.org/10.3991/ijim.v20i02.60139

[27] S. S. Sabry, M. Sahib, and T. Nayl, "Toward hand functions rehabilitation using the virtual world for pre-school children with cerebral palsy," *Int. J. Emerg. Technol. Learn.*, vol. 15, no. 9, pp. 110–122, 2020. https://doi.org/10.3991/ijet.v15i09.13047

11 AUTHORS

Shujiang Zhang is a postgraduate researcher at the Department of Electrical, Electronic, and Systems, Faculty of Engineering and Built Environment, Universiti Kebangsaan Malaysia (UKM), Malaysia. His research interests include wearable IMU systems, gait analysis, human motion assessment, AI agents, large language models, and artificial intelligence applications in biomechanics and rehabilitation (E-mail: zsj3667@gmail.com).

Md. Mahmudur Rahman received the B.Sc. degree in electrical and electronic engineering from Khulna University of Engineering and Technology, Khulna, Bangladesh, in 2007, and the M.Sc. degrees from the Islamic University of Technology, Gazipur, Bangladesh, and the Department of Electrical, Electronic, and Systems, Faculty of Engineering and Built Environment, Universiti Kebangsaan Malaysia (UKM), Malaysia, in 2016 and 2023, respectively. He is currently pursuing a Ph.D. degree with the Department of Electrical, Electronic, and Systems Engineering at UKM. He is on study leave from his position with the Department of Electrical and

Electronic Engineering, Daffodil International University, Dhaka, Bangladesh. His research interests include wearable sensors, biomedical signal processing, artificial intelligence in healthcare, and human motion assessment (E-mail: P138505@siswa.ukm.edu.my).

Xuejin Cao is a postgraduate researcher at the Department of Electrical, Electronic, and Systems, Faculty of Engineering and Built Environment, Universiti Kebangsaan Malaysia (UKM), Malaysia. His research interests include AI-assisted stroke rehabilitation, large language models, explainable AI, and AI agents (E-mail: zhinengmahua@gmail.com).

Kok Beng Gan has received the B.S. degree in Material Physics from University Technology Malaysia in 2001. He was conferred a PhD (Electrical, Electronic & System Engineering) from the Department of Electrical, Electronic, and Systems, Faculty of Engineering and Built Environment, Universiti Kebangsaan Malaysia in 2009. He was an engineer in the field of electronic manufacturing services and original design manufacturing from 2001 to 2005. After several years of industry experience, he decided to venture into academic in 2005. He is currently an Associate Professor in the Department of Electrical, Electronic & Systems Engineering, Faculty of Engineering and Built Environment, Universiti Kebangsaan Malaysia. He specializes in embedded systems and artificial intelligence. His current research interest are artificial intelligence in healthcare, embedded systems & signal processing for medical & industry application, and biomechanics & human motion analysis (E-mail: kbgan@ukm.edu.my).

Kok Swee Sim is currently a Professor with the Faculty of Engineering and Technology, Multimedia University, Malaysia. He actively collaborates with various local and international universities and hospitals. He has filed 23 patents and 85 software copyrights. He is a fellow of the Academy of Sciences Malaysia, the Institution of Engineers Malaysia (IEM), and the Institution of Engineering and Technology (IET), U.K. Over the years, he has received numerous prestigious national and international awards. These include the Japan Society for the Promotion of Science (JSPS) Fellowship in 2018, the Top Research Scientists Malaysia (TRSM) Award from the Academy of Sciences Malaysia in 2014, and the Korean Innovation and Special Awards in 2013, 2014, and 2015. He was a recipient of the TM Kristal Award and multiple World Summit on the Information Society (WSIS) Prizes in 2017, 2018, 2019, 2020, and 2021 (E-mail: kssim@mmu.edu.my).